



# Effect of explosive welding parameters on Al/LCS interface clad by low velocity of detonation explosive welding (LVEW) process

Bir Bahadur Sherpa<sup>1,2,3</sup> · Pal Dinesh Kumar<sup>2</sup> · Abhishek Upadhyay<sup>2</sup> · Sandeep Kumar<sup>2</sup> · Arun Agarwal<sup>2</sup> · Sachin Tyagi<sup>1,3</sup>

Received: 30 June 2020 / Accepted: 8 February 2021 / Published online: 2 March 2021

© The Author(s), under exclusive licence to Springer-Verlag London Ltd. part of Springer Nature 2021

## Abstract

Interfacial properties govern the metallurgical and mechanical behaviour of welded specimens. Hence to study the effect of different parameters on weld interface is an important aspect to bring the desired output properties for various applications. In this study, a newly developed low velocity of detonation explosive welding (LVEW) process was applied to clad aluminium (Al) and low carbon steel (LCS) plates. Loading ratio (R) and stand-off distance (SD) were adopted for this study, as these two mostly affect the welding behaviour and act as important welding parameters. Microstructural examination as well as mechanical tests were performed. Three kinds of morphology were observed at the weld interface, i.e. large waves (LW), small irregular waves (SIW) and smooth flat interface (SFI), where SIW and SFI contribute interface devoid of voids, intermetallic and melting pockets. But at higher R and SD, AlFe and Al<sub>2</sub>Fe intermetallic were observed in non-continuous form in micron range. Elemental analysis confirmed the local diffusion with very thin diffusion thickness of 0.8–2 μm. Micro-hardness profile discloses the shock hardening effects across the vicinity of the weld interface, where an increase in hardness value was above the parent value. Chisel test and shear strength test also confirmed the good quality of bonding, while in shear fracture study, dimple structure was dominated in all the specimens. All these observations concluded that for cladding Al/LCS, LVEW process is best suitable and further, the practicability of these welded plates was checked by fabricating components like bi-metallic O-ring (push-fit type), hollow cylinder and bolts.

**Keywords** Explosive welding · Loading ratio · Low velocity of detonation · Mechanical testing

## 1 Introduction

Aluminium and steel are extensively known for low density and high specific strength, good electrical conductivity, reflectivity, thermal conductivity and corrosion resistance [1–3]. This bi-metallic component has a great demand and wide applications in the marine industry, oil industry, automotive, nuclear fusion engineering, aerospace and shipping industries [1, 4–7].

But welding of this combination by conventional means is challenging due to wide differences in various physical properties of both the materials. Specifically, steel density is almost 3 times that of aluminium and the melting temperature double that of aluminium. These differences either leads to difficulty in joining process itself or results in the formation of intermetallic and thus affects the bond quality [8–11]. Therefore, to circumvent these limitations, explosive welding is preferred as one of the most suitable joining techniques, in which energy of explosive is used as a source of joining two dissimilar metals at atomic level [2, 12, 13]. It is a solid-state joining technique where explosive is detonated with the help of detonator and the detonation wave travels across the plates [14, 15].

During the explosive welding process, jetting phenomenon occurs by high impact of flyer plate on the base plate and it is considered as one of the important criteria for defining good bond. Jetting phenomenon depends on the high temperature and the molten area. To analyse the jet flow and molten area, Zeng et al. studied the extracted melted particles and observed

✉ Bir Bahadur Sherpa  
sherpa7419@gmail.com

<sup>1</sup> Academy of Scientific and Innovative Research (AcSIR), Ghaziabad 201002, India

<sup>2</sup> Terminal Ballistics Research Laboratory (TBRL), DRDO, Sector-30, Chandigarh 160030, India

<sup>3</sup> Central Scientific Instruments Organisation (CSIO), CSIR, Sector-30, Chandigarh 160030, India

that high cooling rate was produced as the effect of thermal conduction and inhibited the melting when the magnitude of Fourier coefficient is higher than  $10^{-7}$  [16]. During the explosive welding process, kinetic energy transformed to thermal energy which causes the adjoining surface metals to get partially melted. As a result of these melted metals, when high pressure is exhausted, a thin oxide film is swept away from the top surfaces of the two materials leaving behind virgin and clean surfaces to form a strong metallurgical bond [17, 18]. Further in explosive welding, the bond quality of welded samples depends on weldability parameters such as stand-off distance (SD), explosive loading ratio (R) and velocity of detonation (VoD), relative position of flyer and base plate, interlayer thickness, etc. [19–21]. For the practical application of these welded plates, proper selection of welding parameters is crucial as too high value of these parameters can lead to intermetallic or defects at bonding interface and too low values can cause improper joining of plates. Various authors have joined Al/Steel bi-metal using explosive welding technique and studied the effect of different welding parameters on bond quality [4, 22–24]. Carvalho et al. explosively welded stainless steel to aluminium alloys and examined the effect of physical properties of materials and their relative position as base and flyer plates to achieve a sound weld joint. The authors observed that proper joining of aluminium steel bimetal was achieved when steel was chosen as a base plate. When steel was used as a flyer plate no bonding was observed as the tensile stress reaches at the interface before the complete solidification of the localized melting. Moreover, very low thermal conductivity of SS as a flyer plate compared to the aluminium base plate leads to the dismantling of these joints [25]. Y. Kaya studied the effect of loading ratio on Al/steel weld using Elbar-5 explosive with VoD of 3000–3200 m/s [4]. M. Acarer and B. Demir also investigated the effect of Elbar-5 explosive on the mechanical properties of aluminium/dual-phase steel bimetal [26]. While M. Yang et al. studied the meshing interface of Al/SS to increase the mechanical properties of the bonding interface using emulsion explosive with VoD 2500 m/s [27]. Although various authors have worked on aluminium steel bi-metal but joining of this combination is still a big challenge especially due to the formation of intermetallic compound (IMC) at the weld interface which lower down the mechanical properties. IMC at the weld interface increases the solidification time of the molten layer which thereby decreases the weldability of Al-steel plates. Therefore, it is desirable to reduce the formation of different intermetallic phases at the weld interface to produce sound joints. In this regard, authors have applied different approaches to minimize the intermetallic formation, an immediate reference is to the work reported by Aceves et al. who used the concept of interlayer in the explosive welding process due to difficulties in direct joining of Al 6061 to 304 SS. They examined the effect of three different interlayers (Ti, Cu and Ta) and explored the properties of explosively welded aluminium/steel

plates for cryogenic pressurized hydrogen storage application. They concluded that Ti and Ta as interlayers have sufficient joint strength and ductility compared to Cu. While Cu as interlayer forms a joint which fails at lower ductility at Al/Cu interface [28]. Carvalho et al. also studied the effect of interlayer in which they explosively welded aluminium to stainless steel using two different interlayers, i.e. carbon steel and niobium. When the two interlayers were analyzed and compared, both showed the favourable interfacial microstructure but the joint using carbon steel interlayer was better in terms of mechanical properties as compared to niobium interlayer [29]. Shiran et al. investigated the effect of heat treatment on the intermetallic compounds of explosively welded steel/aluminium. They observed that the thickness of intermetallic layer was increased from 118.8 to 135.4  $\mu\text{m}$  when the heat treatment duration increased from 6 to 8 h at constant temperature 450 °C. Whereas a decrease in the thickness of intermetallic layer was observed from 118.5 to 104.5  $\mu\text{m}$  by decreasing the heating temperature from 450 to 350 °C [30]. As discussed above, interlayer help to reduce the intermetallic formation but at the same time selection of interlayer is very critical. While selecting the interlayer, composition as well as thickness of the interlayer play a very significant role. As an improper selection of interlayer may bring undesirable effects and also hamper the mechanical properties of the bimetallic plates [31]. Some previous studies concluded that low VoD explosives are more appropriate for defect free joining of dissimilar bi-metals. Recently, Carvalho et al. have also joined Al-Steel combination by taking different VoD ranging from 2072–3514 m/s and witnessed very small pockets as well as the formation of molten layer was reduced by using low VoD explosive [32]. At low VoD conditions, dissipation of kinetic energy at the collision point is lower which can result in sound welds with strong metallurgical bonding. Moreover, when VoD is very high it will produce high shock waves across the weld material, which will generate tensile stresses sufficiently high to destroy already established bonds. The detonation velocity of most of the explosives lies within range of 6000–7000 m/s and the velocity of sound in metals found between 2000 and 6000 m/s. To obtain a sound weld the collision velocity ( $V_c$ ) which is equal to detonation velocity ( $V_d = \text{VoD}$ ) for parallel configuration, should not exceed the velocity of sound in either of the participant metal. Although research work has been conducted for Al-steel combination, influence of different process parameters on the weld interface in low VoD conditions ( $< 2000$  m/s) is still unexplored. Therefore in this present study, the low velocity of detonation explosive welding (LVEW) process is exploited to weld aluminium to steel under different welding conditions, i.e. at different loading ratio and stand-off distance and the welded plates were characterized rigorously in terms of microstructure and mechanical behaviour across the weld interface.

## 2 Material and methods

In the present work, Al (300 mm × 150 mm × 5 mm) as flyer plate and LCS (300 mm × 150 mm × 19 mm) as the base plate were joined using low velocity of detonation explosive welding (LVEW) process. Low velocity of detonation explosive (LVE-1) mixture having VoD less than 2000 m/s and density of 800 kg/m<sup>3</sup> was used [33]. Five Al/LCS composite plates were manufactured at different loading ratio and stand-off distance. Parameters of all the samples (1–5) are given in Table 1. The chemical composition and the mechanical properties of the flyer and base plates are given in Tables 2 and 3, respectively. The parallel setup was used during the welding process where the two plates to be welded are placed parallel to each other separated by stand-off distance. The schematic of low VoD explosive welding (LVEW) process is shown in Fig. 1 in which the whole procedure is described. Also, the actual experimental setup is shown in Fig. 2 for better clarification and understanding of the experiment.

### 2.1 Kinetic energy dissipation

On detonation of the explosive, the chemical energy stored in explosive gets converted into the kinetic energy which forces the flyer plate to impinge into the base plate, causing metallurgical cladding of the two plates. At the collision point, the kinetic energy of the flyer plate is converted into heat energy [34]. The dissipation of the kinetic energy at the interface plays an important role in the bond formation as this energy dissipation results into melting at the interfacial zone during the collision. The amount of kinetic energy loss due to the collision is expressed by Eq. 1 [35].

$$\Delta KE = \frac{m_D m_C V_p^2}{2(m_D + m_C)} \tag{1}$$

where  $m_D$  is the mass of the flyer plate per unit area,  $V_p$  is the flyer plate velocity and  $m_C$  is the mass of the collided

plate per unit area. In this research work, five samples of Al/LCS were prepared at different  $R$  and  $SD$ , and then effect on the interface was analysed based on loss in kinetic energy ( $\Delta KE$ ).

### 2.2 Interface characterization

#### 2.2.1 Metallographic analysis

Specimens from welded plates joined under different experimental conditions were cut parallel to the explosive direction to reveal and analyse the microstructure of the welded interface of composites. These samples were grounded with emery grades starting from coarser (120) till finer one (2000). The morphological and microstructural variations due to different impact loading in the welded interface were observed through a scanning electron microscope (SEM). Along with this, elemental analysis in terms of line and dot mapping was performed to study the behaviour of elements across the weld interface through energy dispersive spectroscopy (EDS) (Model Carl ZEISS, USA, EVO15).

#### 2.2.2 Mechanical tests

To analyse the change in mechanical properties of the explosively welded plates, various mechanical tests were carried out. To check the variation of micro-hardness across the welded interface, Vickers micro-hardness tester (Model- Radical, India, RMHT201) with a load of 0.1 kg and dwell time of 15 s was used. For which, series of indentations were made at regular intervals of 200 μm distance across the interface till 1000 μm distance on either side of Al and LCS interface. To evaluate the mechanical strength of the welded specimens, shear testing was carried out as per standard DIN 50612. In this test, the compressive load was applied gradually at the weld interface of Al/LCS using Universal Testing Machine (UTM) with a

**Table 1** Selected parameters for explosive cladding

	Welds				
	Sample 1	Sample 2	Sample 3	Sample 4	Sample 5
Flyer plate	Aluminium	Aluminium	Aluminium	Aluminium	Aluminium
Base plate	LCS	LCS	LCS	LCS	LCS
Configuration	Parallel	Parallel	Parallel	Parallel	Parallel
Explosive	Trimonite + salt	Trimonite + salt	Trimonite + salt	Trimonite + salt	Trimonite + salt
Flyer thickness	5 mm	5 mm	5 mm	5 mm	5 mm
Base thickness	19 mm	19 mm	19 mm	19 mm	19 mm
Explosive ratio	0.6	0.8	1.0	1.2	1.4
Stand-off distance	5.1 mm	6.1 mm	7.1 mm	8.1 mm	9.1 mm

**Table 2** Chemical composition (wt. %) of low carbon steel and aluminium

Materials	C	Si	Mn	S	Mg	P	Cu	Cr	Fe	Al
LCS	0.21	0.17	0.68	0.13	-	0.27	-	0.16	Bal.	-
Al	-	0.179	0.0224	-	0.0673	-	0.122	-	0.494	Bal.

**Table 3** Mechanical properties of participating materials

Materials	Vickers hardness value (measured HV)	Melting point (K)	Density (kg/m <sup>3</sup> )	UTS (MPa)	Thermal conductivity (W/mK)	Specific heat (J/kg K)
LCS	157	1789	7800	340	51.1	486
Al	40	928	2700	90	235	904

capacity of 60 kN, until the joints get shear off. The testing fixture, specimen and mode of loading are designed such that the bonded area is subjected to shear stress leading to failure at the interface of the weld. Another qualitative but rigorous test known as chisel test was also done to check the bond strength at the interface of welded joints for all the samples. Along with this, fracture study was carried out using SEM and EDS to observe the morphology of the shear strength test fracture.

### 3 Results and discussion

The prime objective of this work is to analyse the effect of different welding parameters (loading ratio and stand-off distance) on weld interface of aluminium-steel bi-metal joined by a newly developed low velocity of detonation explosive welding process (LVEW). The microstructural and mechanical behaviour of Al-steel bi-metal in low-energy conditions is as follows:

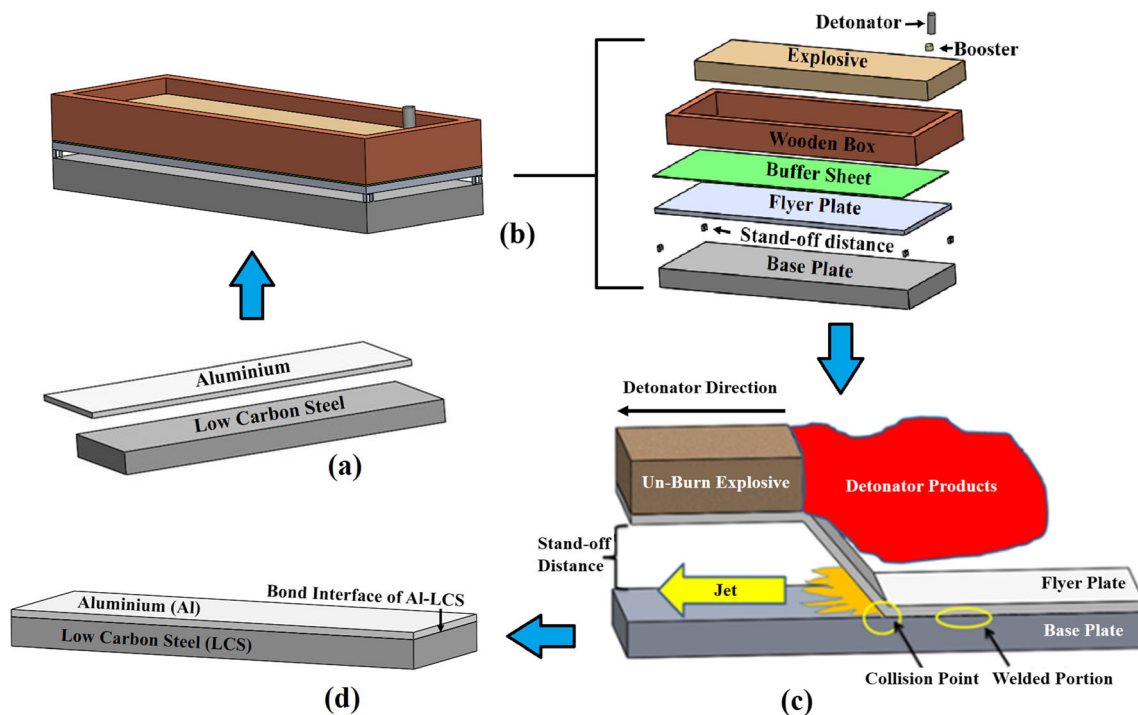


**Fig. 1** Schematic view of the LVEW process: (a) represents the plates before the trial, (b) elaborated view of the setup shown for clear visualization of the process, (c) cladding of plates when explosion has initiated, and (d) explosively welded plate

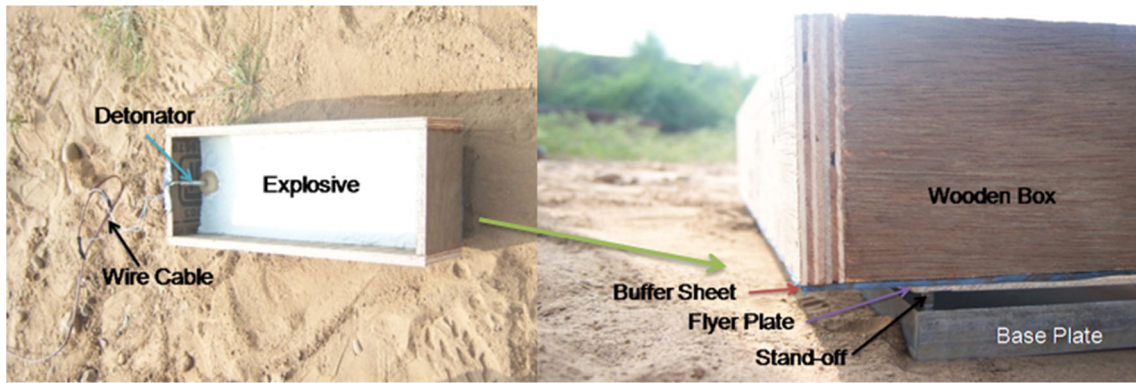


Fig. 2 Practical experimental setup

### 3.1 Microstructural characterization

SEM images showing microstructural behaviour at the interface of welded samples are presented in Figs. 3 and 4. Translation of interface morphology from smooth to the wavy was observed with an increase in  $R$  and  $SD$  values. These translations can be attributed to the upsurge in deformation rate due to increased flyer plate velocity ( $V_p$ ) and pressure at

high energetic conditions [36, 37]. At higher loading ratio conditions (sample 5), shown in Fig. 3 (a and a'), large waves (LW) were observed along with some island of melt layers across the weld interface. The morphology of the weld interface also reveals some small irregular waves (SIW) across the joints for sample 4 with no melt layers. For samples 2 and 3 shown in Fig. 4, small irregular waves (SIW) along with smooth flat interface (SFI) were found across the weld

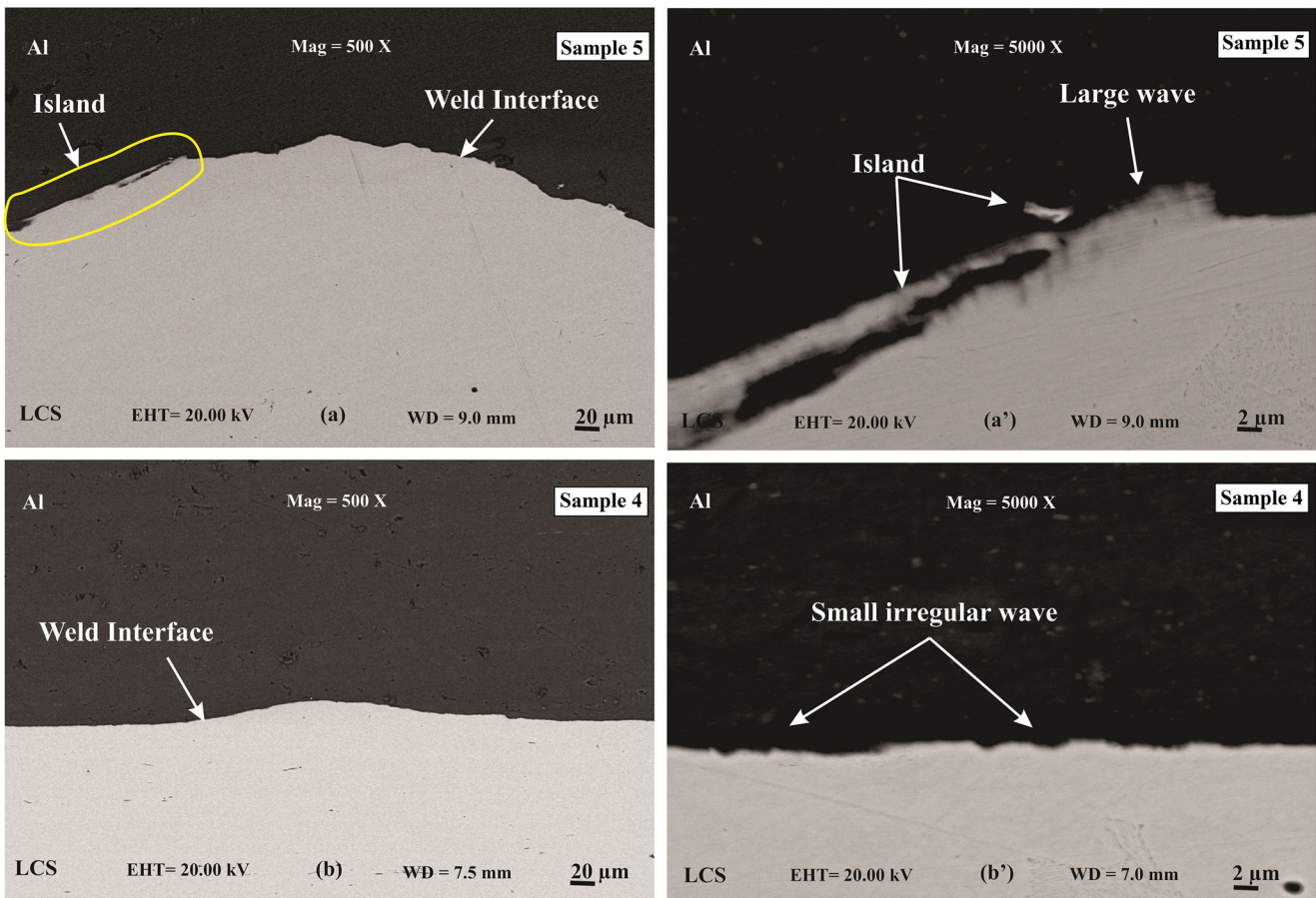
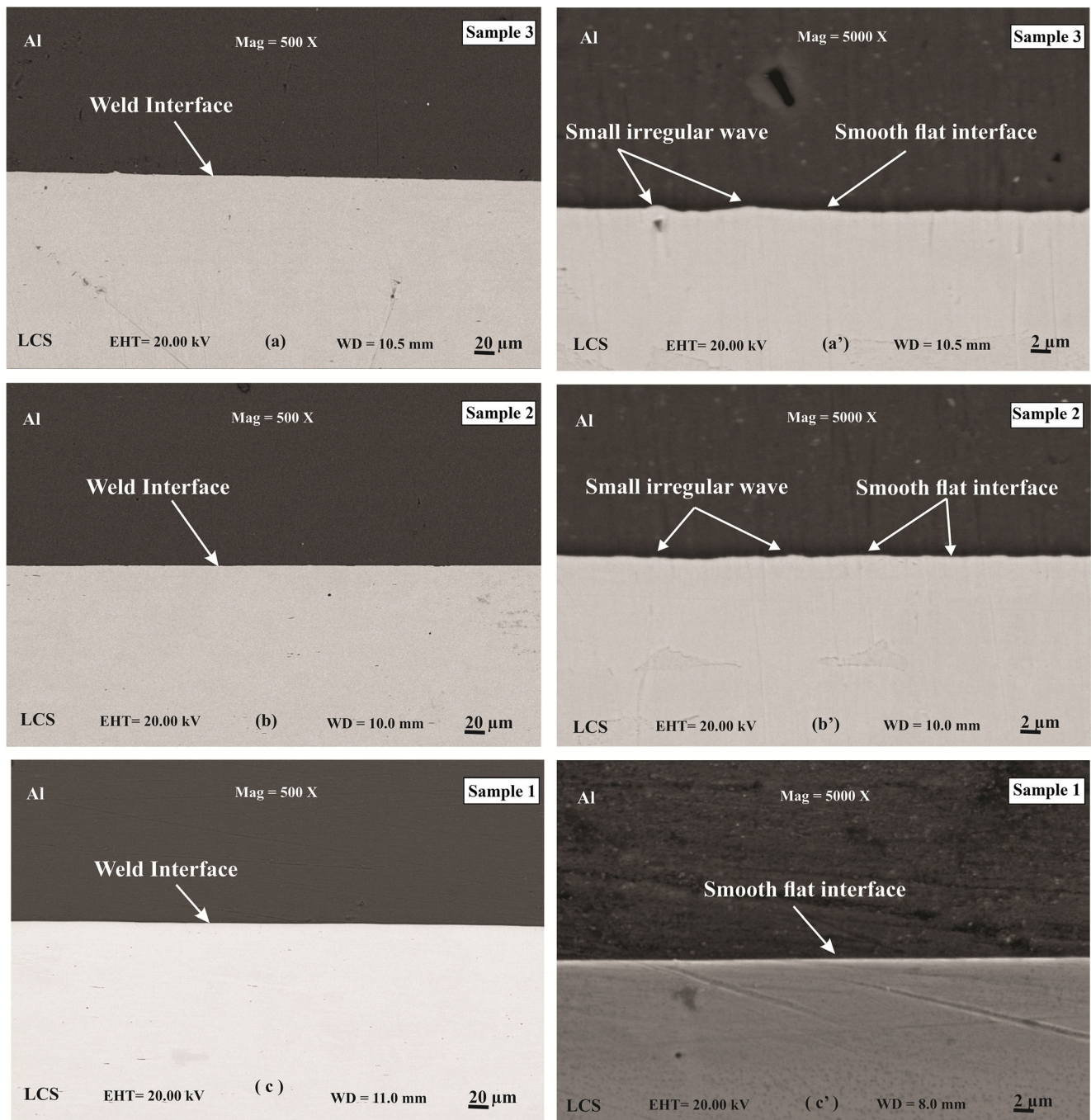


Fig. 3 SEM micrographs at different loading ratio and magnification: a sample 5 with 500X, (a') sample 5 with 5000X, b sample 4 with 500X, and (b') sample 4 with 5000X



**Fig. 4** SEM micrographs at different loading ratio and magnification: **a** sample 3 with 500X, **(a')** sample 3 with 5000X, **b** sample 2 with 500X, **(b')** sample 2 with 5000X, **c** sample 1 with 500X, and **(c')** sample 1 with 5000X

interface and only a smooth flat interface (SFI) was observed for sample 1. In the SEM micrographs of samples 1–4, no major defects were observed at the weld interface. Comparing the interface morphology of Al-LCS bimetal obtained in present case with previously reported work, it was observed that smooth flat morphology obtained for samples welded in lower experimental conditions is in great agreement with the observations reported by Carvalho et al. According to the authors, flat morphology without irregularities are

observed with explosive of lowest detonation velocity. From the results, it can be concluded that VoD of an explosive act as a deciding factor for weld interface morphology [32]. The wavy interface morphology at high loading ratio and stand-off distance are not in good agreement with conclusions of Carvalho et al. However, Yakup Kaya observed similar transition of interface morphology from flat to wavy with increasing loading ratio suggesting that along with VoD, loading ratio and stand-off distance also affect the morphology of

Al-steel weld interface [4]. Compared to microstructural behaviour of weld interface with other works reported in different VoD range, the weld interface obtained in present case is more regular, devoid of cracks and pockets. Reason for this can be VoD towards lower range compared to previous studies [4, 17, 38, 39]. EDS analysis of island obtained for sample 5 was done by taking four different points as shown in Fig. 5, where the first two points were placed along the island and next two across the interface. The first two points show the presence of Al<sub>2</sub>Fe and AlFe intermetallic in the non-continuous form in the micron range. The next two points presented the same composition as parent materials. This microstructural behaviour at the weld interface can also be explained based on kinetic energy loss during the welding process. During the collision, the loss in kinetic energy largely depends on flyer plate velocity ( $V_p$ ) which in turn correlated to detonation velocity of explosive ( $V_d$ ) as shown in Eq. 2.

$$V_p = V_d \frac{0.612R}{(2 + R)} \tag{2}$$

Here  $R$  is the loading ratio (unit less parameter) and  $V_d$  is the detonation velocity of explosive in m/s. Therefore, low VoD of the explosive mixture leads to decrease down the possibility of intermetallic and vortex formation at the weld interface. Kinetic energy loss for all experimental conditions was calculated using Eq. 1 and correlated with the morphology of the interface. Values of  $\Delta KE$  obtained for different samples are given in Table 4. For sample 1, the value of  $\Delta KE$  is 1.51 MJm<sup>-2</sup> which increased to 4.45 MJm<sup>-2</sup> for sample 5. From the obtained results, it was observed that at lower kinetic energy loss conditions, the morphology of the interface is smooth and at higher kinetic energy loss conditions morphology of the interface is wavy as the reaction between the materials increased at high kinetic energy conditions which causes a high rate of plastic deformation. This phenomenon was also observed by P. Manikandan that the microstructural changes are directly affected by the plastic deformation caused by kinetic energy loss [40]. Shiran et al. also witnessed that with an increase in stand-off distance the thickness of the intermetallic layer has increased which

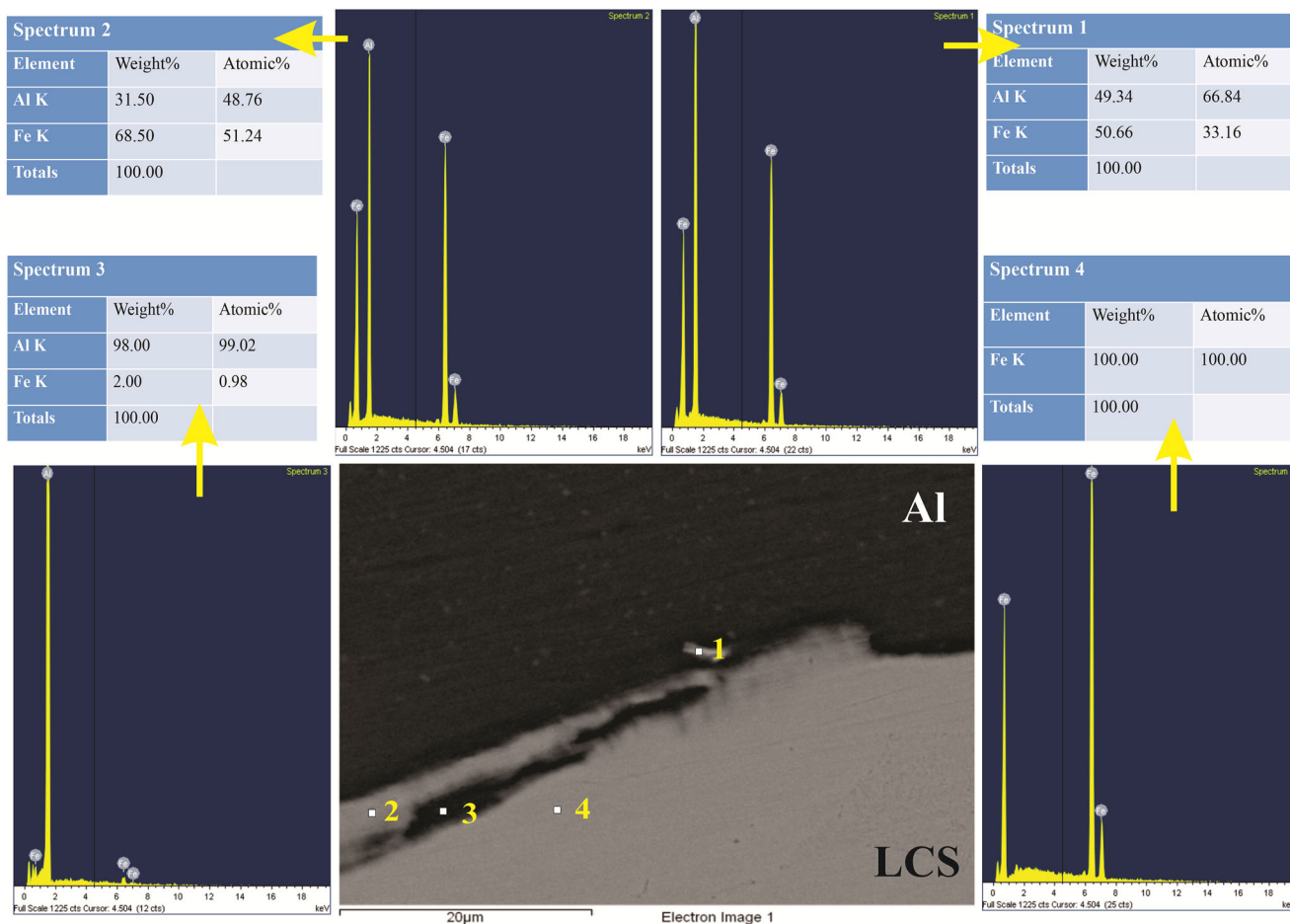


Fig. 5 SEM micrographs with EDS analysis for sample 5

**Table 4** Kinetic energy loss at different loading ratio conditions

Sample no.	Loading ratio ( $R$ )	Stand-off distance (mm)	Kinetic energy loss $\Delta KE$ ( $MJm^{-2}$ )
1	0.6	5.1	1.51
2	0.8	6.1	2.24
3	1.0	7.1	2.98
4	1.2	8.1	3.72
5	1.4	9.1	4.45

was due to intense plastic deformation caused by an increase in kinetic energy [30].

### 3.1.1 Elemental analysis

Elemental analysis of Al and Fe using EDS was performed to show the distribution of participant elements across the clad interface. The concentration profiles of Al and Fe in terms of line and dot mapping across the Al/LCS bimetallic are shown in Fig. 6 (samples 5 and 4) and Fig. 7 (samples 3–1). The obtained results (samples 4–1) show that the content of Al and Fe remained constant, while for sample 5, there was some kind of un-even slope in the content of Al, which is due to the presence of some intermetallic component. For all the samples, there was a trend of forming “X” shape in line maps by

the two elements. This trend of X-shape formation is one of the indications that the diffusion phenomenon has occurred. Similar diffusion behaviour can also be observed for dot mapping.

In the current work, very small diffusion layer was observed with a minimum range of 0.8  $\mu m$  and a maximum of 2  $\mu m$ . This minor diffusion has occurred mainly due to the microsecond time duration of the process due to which there was no sufficient time to form a thick diffusion layer. Simultaneously, occurrence of high temperature and pressure during high-impact process at the collision point trigger and promote the atoms near the surface to share their orbits and diffused into one another [41, 42]. Collision velocity plays an important role as observed by Zerui Sun et al. in their study. At high collision-speed, diffusion thickness of 4–5  $\mu m$ , and at

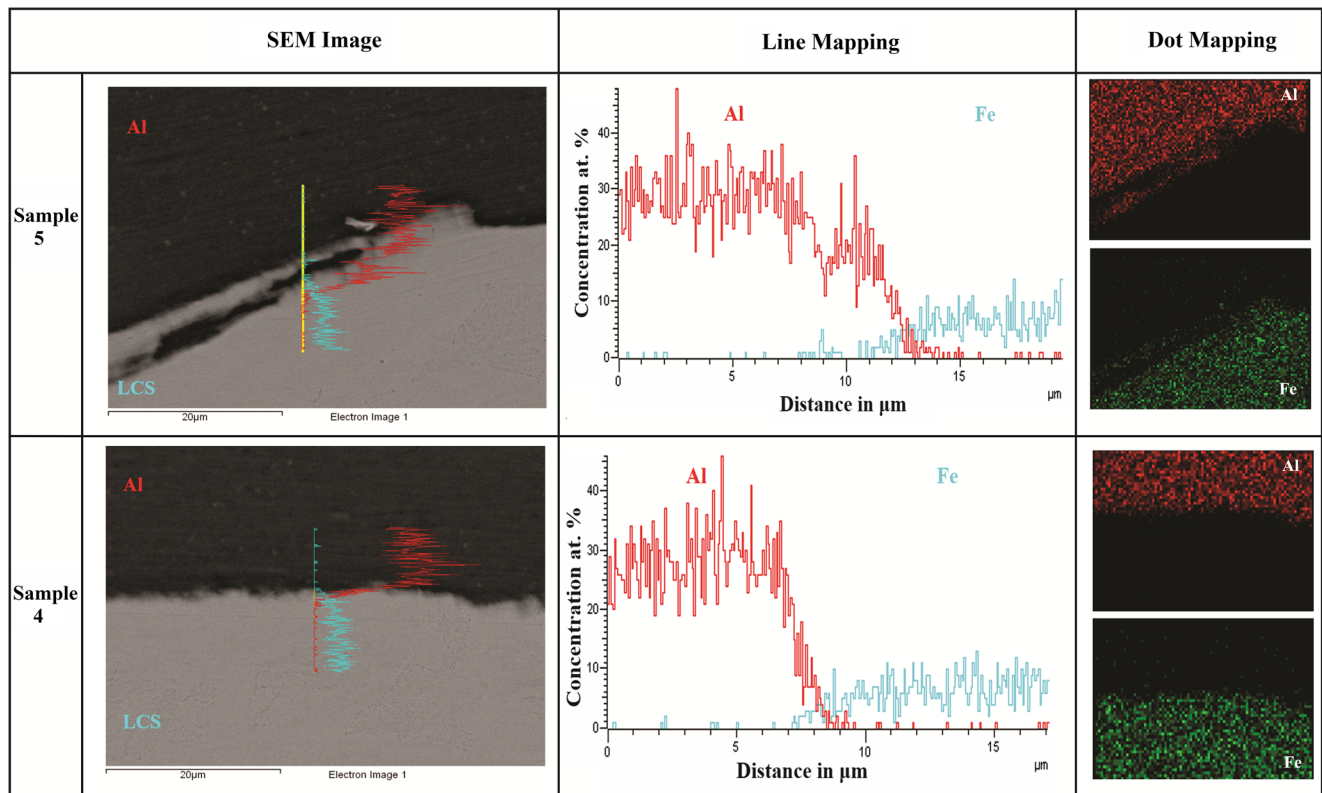


**Fig. 6** SEM image of Al/LCS for samples 5 and 4 with EDX map analysis showing the distribution of Al and Fe (line and dot mapping)



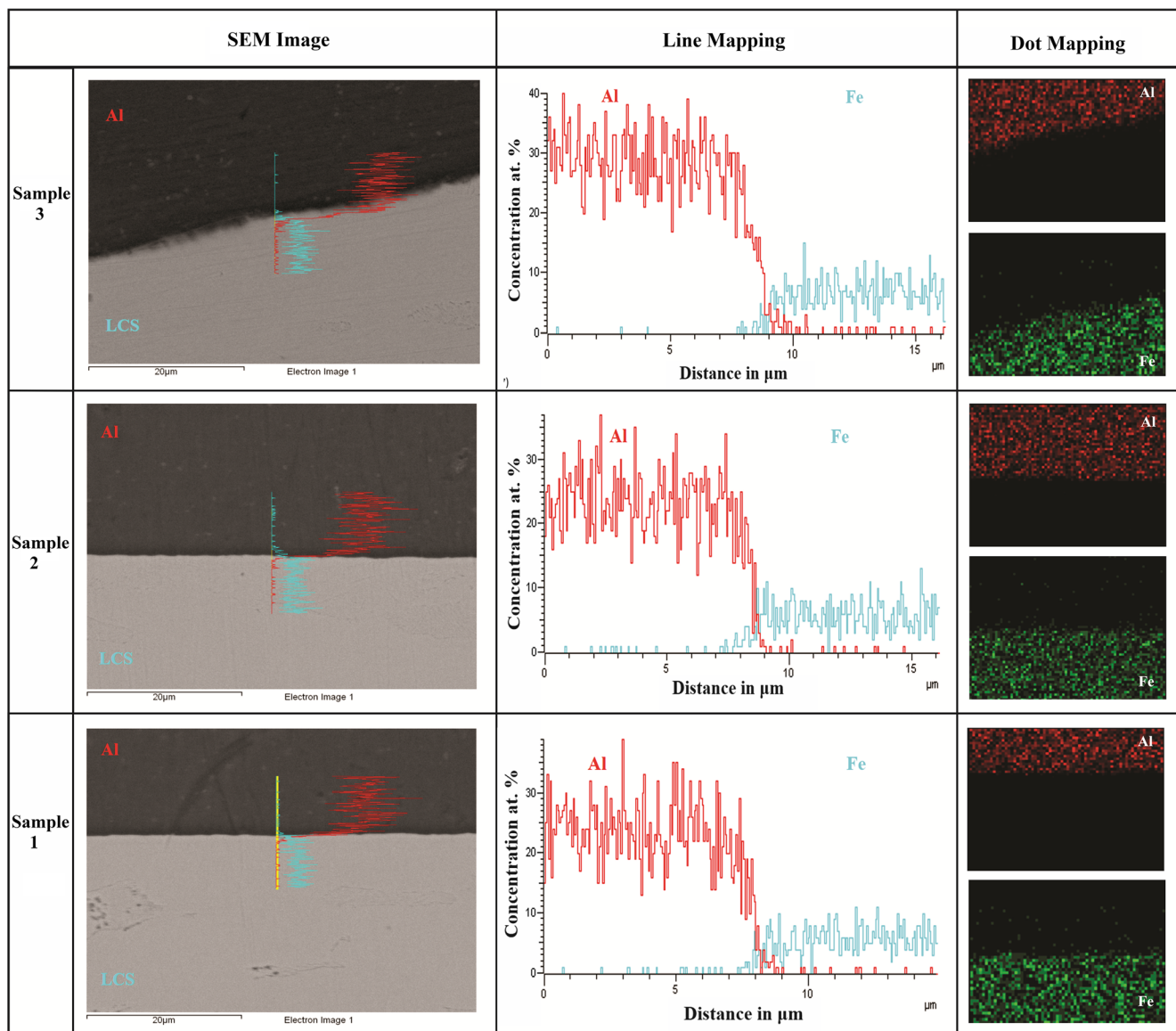


**Fig. 7** SEM image of Al/LCS for samples 3–1 with EDX map analysis showing the distribution of Al and Fe (line and dot mapping)

low collision speed, the diffusion thickness of 2–2.5  $\mu\text{m}$  across the interface was obtained. It was observed that the atoms near the interface become more active and efficient at higher collision speed [43]. Ye Cui et al. observed diffusion thickness of 3  $\mu\text{m}$  and 1  $\mu\text{m}$  across the Ti/steel bimetallic combination, when they applied the detonation velocity of 2100 m/s [44]. In the current study, the diffusion thickness was approximately 0.8–2  $\mu\text{m}$ , which can be resulted due to LVEW process as temperature and pressure generated was low and hence the diffusion across the interface was very small. As higher the diffusion layer thickness, chances of formation of intermetallic compounds increases. Sun et al. explosively welded bimetallic samples at different collision speeds and observed that at higher collision speed, the atoms near the weld interface become more efficient and active during

diffusion. More heat is generated at higher collision speeds which resulted in more intermetallic compounds [43].

## 3.2 Mechanical testing

### 3.2.1 Micro-hardness examination

The micro-hardness test was performed and the hardness profiles near the weld interface are presented in Fig. 8. The maximum increase in hardness value was observed near the weld interface, which is due to the work hardening process. The work hardening was caused by the high impact of flyer plate over the base plate during LVEW process and can be observed that the effect of work hardening get decreased as the distance from the weld interface increases. In the current work, for

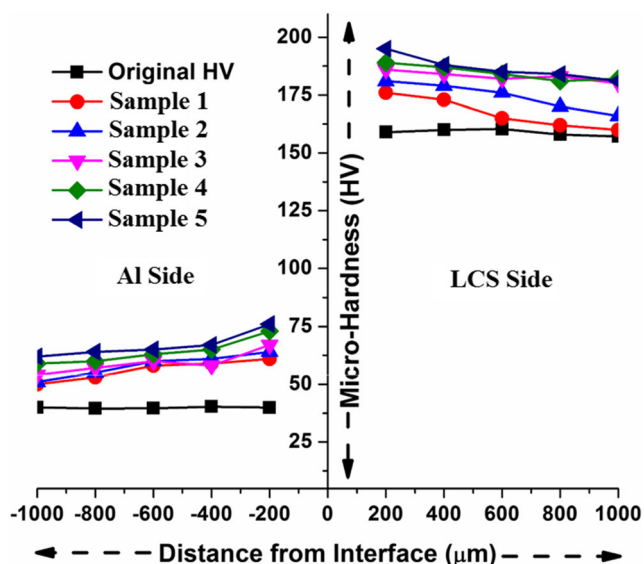


**Fig. 8** Micro-hardness profiles of different samples at the interface of welded plates

sample 5, the hardness values of Al and LCS increase from base value 40 HV and 157 HV to a maximum value of 76 HV and 195 HV, respectively. This increase in hardness value was almost twice for Al as compared to LCS, which shows that the flyer plate has experienced higher impact than the base plate. Similar results were also witnessed by Athar and Tolaminejad in which they observed a two-fold increase in hardness value for Al compared to Cu [45]. Comparing the results with the published work, the present observations concur with Yakup Kaya where an increased in hardness value was noticed with the increase in explosive loading ratio. Author concluded that with increase in loading ratio, impact velocity of the plate increases and as a result deformation level increases. Therefore, this increase in deformation cause an increase in hardness value near the weld interface [4]. Similarly, Kaya and Eser also observed an increase in hardness value, where they concluded that the increase in hardness was due to the cold deformation and grain refinement near the weld interface caused by high impact pressure at high velocities during the explosion [46]. Yang et al. also observed similar trend at the weld interface of Al-steel bimetal and concluded that the behaviour was due to work hardening caused due to plastic deformation at the weld interface [27]. Recently, using micro-hardness values Sherpa et al. developed a model based on adaptive network-based fuzzy inference system (ANFIS) to predict the micro-hardness value at the weld interface of Al/LCS, where the micro-hardness value predicted through the ANFIS model was found to be in good agreement with the experimental hardness values [47]. Comparing the two materials across the weld interface of Al/LCS bi-metal, the maximum hardness was observed at LCS side. This increase in hardness was due to higher strain hardening of LCS with respect to Al. Comparing the overall hardness values, it was

observed that micro-hardness value was directly proportional to  $R$  and  $SD$ .

### 3.2.2 Chisel test

To examine the bond strength of the welded specimens, chisel test was performed. This test is one of the qualitative but rigorous tests to check the strength of the bonded specimens, in which manual force is applied at the weld interface. Figure 9a shows the welded specimen hold in a vice and subjected to chisel test, and Fig. 9b shows failure in the welded specimen after chisel test. SEM analysis of the failure region obtained during chisel test was also carried out and shown in Fig. 9c, d. It was observed that the adherence of Al layer was less at lower welding conditions (sample 1) compared to higher conditions (sample 5), which is possibly due to higher bond strength of Al/LCS interface in case of higher loading ratio. SEM results (for all  $R$  and  $SD$ ) revealed that the joint was not separated from the interface; rather, failure has been observed on the Al side in all the samples. This also gives the observation that the failure occurred from the material having weaker strength (flyer plate). Else the material has been failed from the weld interface if the bond so formed was not strong. But in the present study, in all the welded specimens, the material got chipped out from the Al side slightly above the weld interface, which shows the presence of a strong metallurgical bond. This observation can also be correlated with the elemental study performed in Sect. 3.1.1, which shows the two materials got diffused into one another during LVEW process.

### 3.2.3 Shear test evaluation

The specimens used for the shear test (samples before and after the test) along with results are shown in Fig. 10. Throughout the shear strength test, the failure followed the same pattern, in which failure occurred from the Al side, which shows that the shear strength at the weld interface is higher than the measured shear strength value. The shear strength obtained from the test is shown in Fig. 10c, where it can be observed that the results obtained for all the specimens have acceptable shear strength value. These results confirm strong interlocking between the flyer plate and the base plate during the explosive welding process. Minimum and maximum shear strength values of 105.0 MPa and 126.2 MPa were observed for samples 1 and 4, respectively. But due to the presence of intermetallic phases at the weld interface of sample 5, there was a slight decrease in strength value. Similar kind of results were also witnessed by Athar and Tolaminejad where an increase in shear strength was associated with higher loading ratio and impact velocity. As under higher loading ratio wavy morphology is obtained which increases bonding surface area and helps in improving the mechanical locking

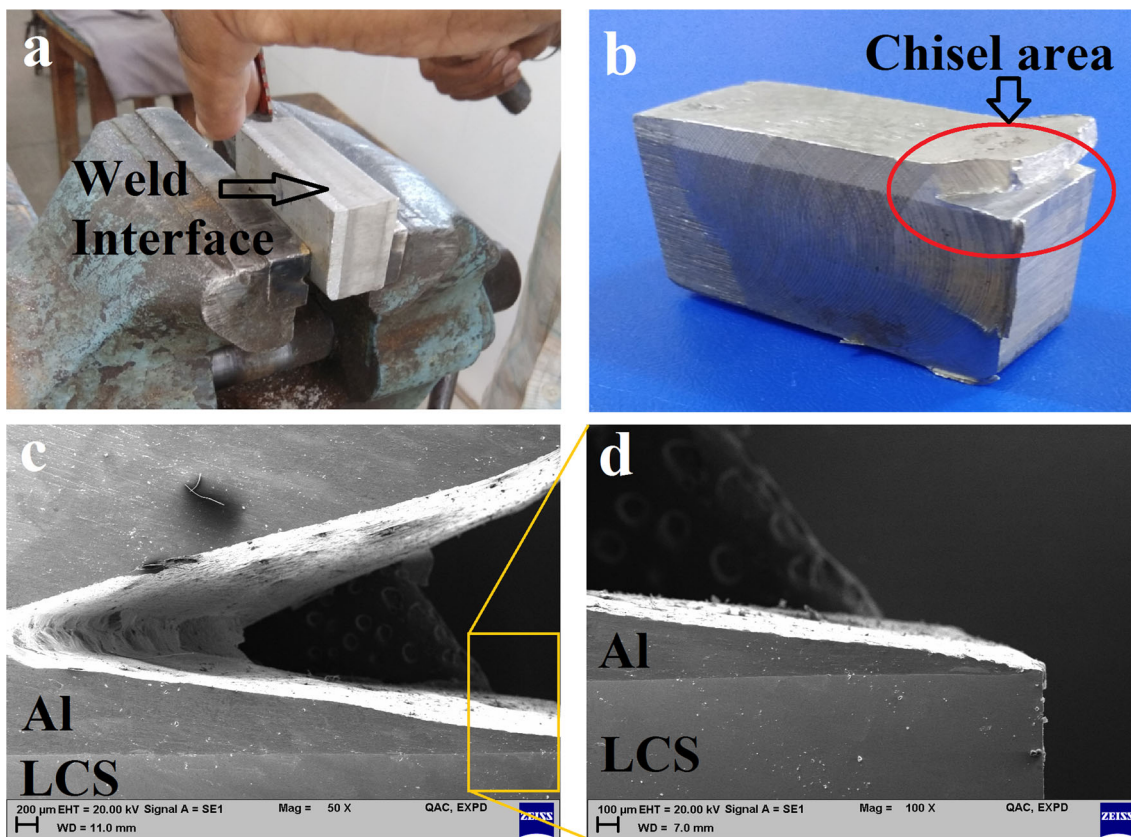


Fig. 9 Specimen before Chisel test (a), and after Chisel test (b), SEM image of specimen after Chisel test at 50X (c), SEM image of specimen after Chisel test at 100X (d)

between two bimetallic plates [45]. Kaya and Eser in their study also experienced an increase in shear strength value with increase in loading ratio conditions [46]. Comparing the obtained shear strength values of all the samples, it was observed that it was higher than weaker parent material, i.e. aluminium.

When compared with other researchers’ work, similar trend was observed [48, 49]. Li et al. when used VoD of 2122 m/s and performed explosive welding of aluminium and steel, observed shear strength greater than the base material [22]. Yakup Kaya when applied VoD 3000–3200 m/s for explosive

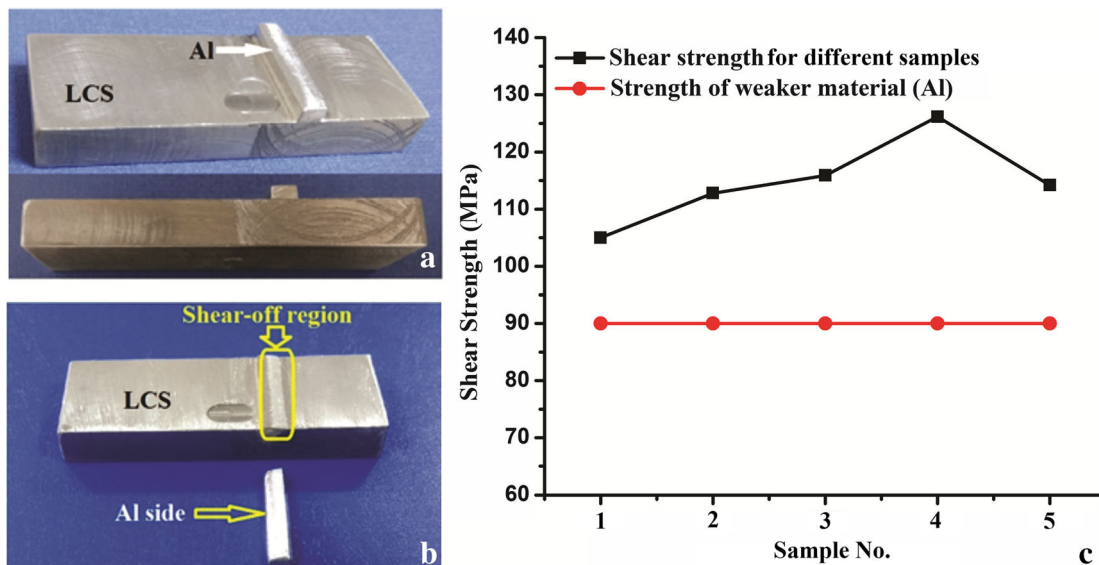


Fig. 10 Shear strength specimens (a) before and (b) after the test (c) hear strength values for sample 1-5

welding steel and aluminium, observed an increase in shear strength value with increase in loading ratio but the strength obtained was not higher than the base material [4].

### 3.2.4 Fracture analysis

The micromorphology of the shear fracture as investigated by SEM and EDS is shown in Fig. 11. In all the samples numerous cup-like depressions and elongated dimple structures can be observed. Mastanaiah et al. in their study also observed similar fractured samples with dimple rupture [49]. These dimple structures are usually formed during the shear phenomenon. As during fracture, the material goes under plastic deformation due to applied stress, which results in the formation of micropores at the interface. These micropores developed gradually with the increase of stress level until the ma-

terial get fractured [50]. Wang et al. have discussed in their study that the shape of shear dimples change with the stress conditions. Equiaxial dimples are formed under normal stress and the dimples extend along the shear direction to form elongated dimples under the shear stress [51]. It can be observed from Fig. 11 that for sample 1, the size of the elongated dimple was small as compared to sample 5, which implies that more plastic deformation has occurred with an increase of loading ratio and stand-off distance. These kinds of elongated dimples also indicate that a large amount of energy was absorbed before failure at high loading ratio conditions. Where for sample 5, along with elongated dimples some unambiguous cleavage fracture was also witnessed, which can be attributed to intermetallic formed in this sample as discussed in Sect. 3.1 and also due to high degree of shock hardening phenomenon [52]. In all the specimens, mostly elongated dimples have dominat-

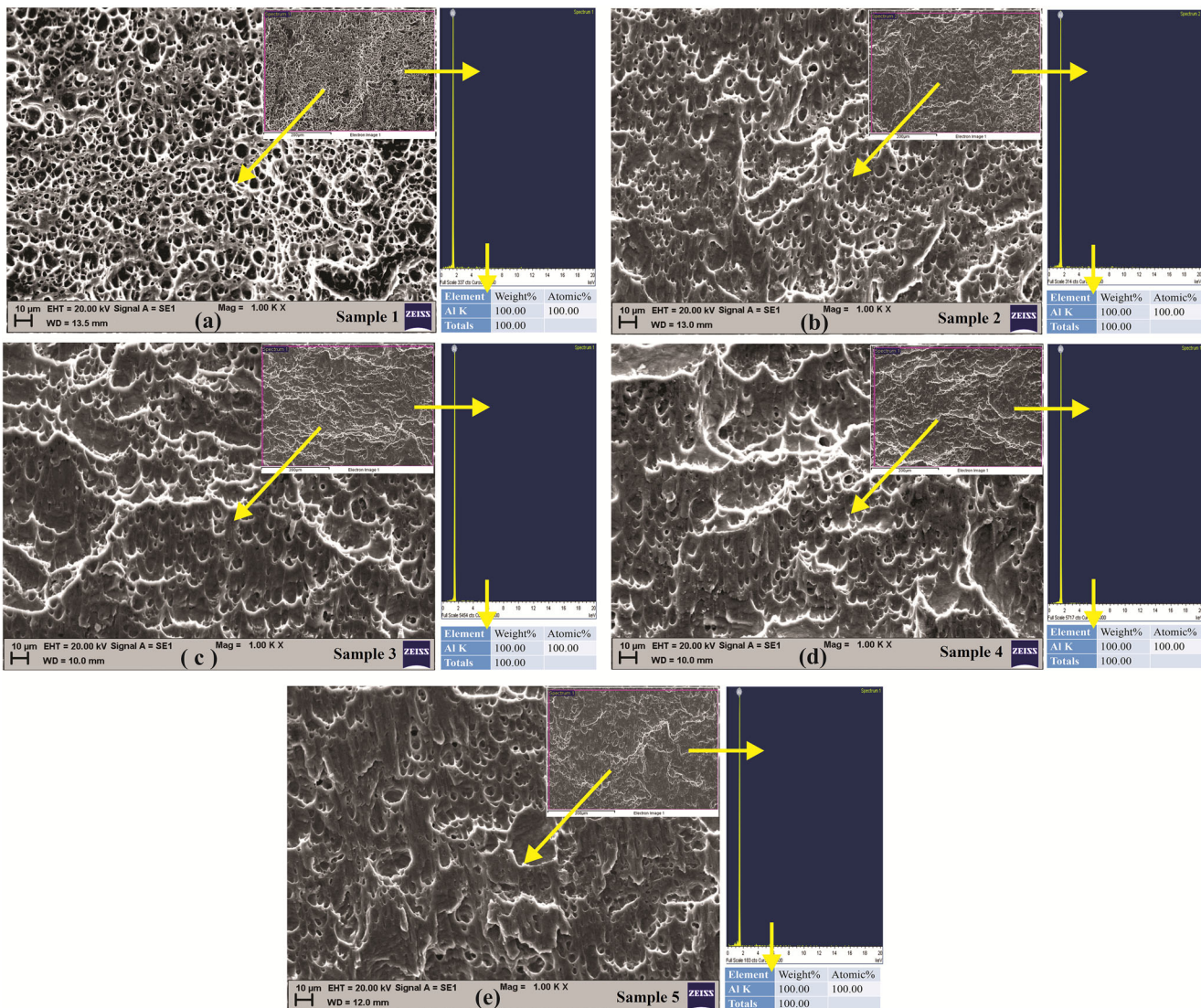


Fig. 11 Fractography after the shear test for samples 1–5

ed and found in majorities confirming ductile nature of the failure. EDS analysis of shear samples was also performed for further visualization of shear fracture. It was observed that all the samples exhibited 100% aluminium in chemical composition. EDS results also support that the fracture has occurred from the aluminium side demonstrating strong bond formation across Al/LCS weld interface in all the samples. Comparing with the other reports, similar kind of dimple structure and ductile fracture were also observed by Li et al. and Yang et al. in fractography study of Al-steel sample [22, 27].

### 3.3 Fabrication of explosively welded products

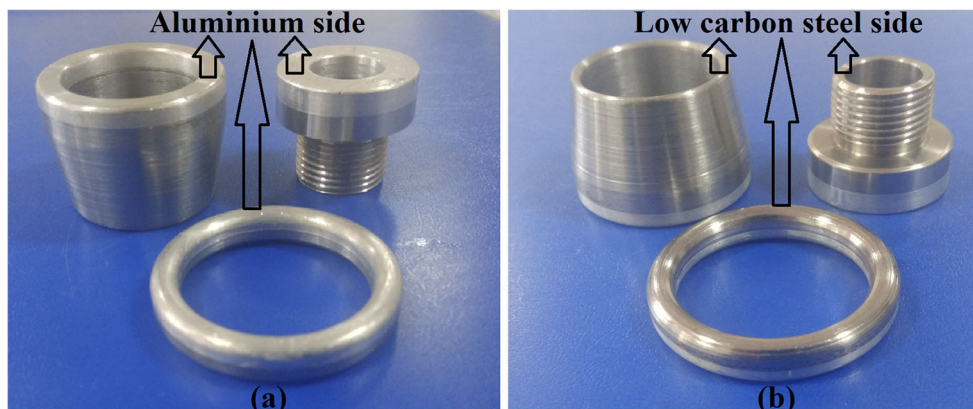
Explosive welding is one of the promising joining techniques and offers a solution to produce bimetals for practical applications such as fabrication of transition joints for cryogenic applications, marine applications and applications related to use of bi-metallic components in ship-building [1, 28]. In this regard, it is worth mentioning that different configurations of components were fabricated from the Al/LCS plates which were being joined during this experimental study. This practical aspect of our experimental study has been realized in the form of actual components that includes bi-metallic O-ring (push-fit type), hollow cylinder and bolts as shown in Fig. 12. Here, Fig. 12a shows aluminium towards the upper side and in Fig. 12b low carbon steel is towards the upper side. These components are further needed to be tested for different applications. During machining, various forces act at the specimens and from the image it can be observed that the welded bimetallic components have overcome such forces. This result also confirms good mechanical strength of welded plates; otherwise, the samples may have dismantled during the machining process. This shows that the bimetallic plates joined through LVEW process are of good strength and can be used for fabrication of different products.

## 4 Conclusions

The objective of present work was to study and analyse the effect of varying loading ratio and stand-off distance on interface morphology (microstructure) as well as mechanical properties of Al/LCS joints welded using a newly developed low velocity of detonation explosive welding (LVEW) process. The important conclusions are as follows:

- Low velocity of detonation explosive welding (LVEW) process is feasible to clad Al and LCS plates with strong metallurgical bonds at all loading ratio and stand-off distance conditions.
- Straight to wavy interface morphology was observed with increasing loading ratio and stand-off distance. Interface morphology is greatly influenced by kinetic energy dissipation which indirectly depends on VoD, loading ratio and stand-off distance. Defect-free interface was obtained for samples 1–4 while interface with high-amplitude waves and intermetallic compounds  $Al_2Fe$  and  $AlFe$  was obtained for sample 5.
- The micro-hardness studies showed an increase in hardness value near the weld and decrease as moving away from the interface in all the samples, which was mainly due to high impact pressure and intense plastic deformation at the weld region. Sample 5 with large-wave (LW) morphology exhibited the highest value of micro-hardness among all the samples.
- Chisel test showed strong bonding in all the five samples as material got chipped from the Al side, rather than weld interface. The obtained shear strength value was higher than that of the weaker material (Al) in all samples. The optimal shear strength was obtained for sample 4. Drop-in shear value was observed for sample 5 due to intermetallic formation. Fracture analysis shows the dominance of dimple structure, while EDS of the fractured samples shows presence of Al only, which confirms that the shear strength at the interface was higher than the measured value, as the material gets sheared from the Al side.

**Fig. 12** Fabricated products of Al-LCS showing (a) Al side and (b) LCS side



- Different components that include bi-metallic O-ring (push-fit type), hollow cylinder and bolts were fabricated. Results show that the LVEW process enables defect-free weld interface with good quality bonding and further can be applied for different industrial and armament applications.

**Acknowledgements** The support from the Terminal Ballistics Research Laboratory is highly acknowledged. Authors are very thankful to Dr. Manjit Singh, Director, TBRL, Sec 30, Chandigarh and all the scientists, technical officer of EED, QAC Lab EXPD, M.T, and workshop of TBRL for their valuable support.

**Authors' contribution** Experimentation: Bir Bahadur Sherpa, Pal Dinesh Kumar, Abhishek Upadhyay, Sandeep Kumar; writing (original draft preparation): Bir Bahadur Sherpa; writing (review and editing): Bir Bahadur Sherpa, Pal Dinesh Kumar, Abhishek Upadhyay, Sandeep Kumar, Arun Agarwal, Sachin Tyagi; supervision: Pal Dinesh Kumar, Sachin Tyagi; coordination: Bir Bahadur Sherpa

**Funding** This work was supported by Terminal Ballistics Research Laboratory (TBRL), Lab of DRDO, Chandigarh, India.

**Availability of data and material** The authors confirm that the data and material supporting the findings of this work are available within the article.

## Declarations

**Ethical approval** The article follows the guidelines of the Committee on Publication Ethics (COPE) and involves no studies on human or animal subjects.

**Consent to participate** Not applicable. The article involves no studies on humans.

**Consent to publish** Not applicable. The article involves no studies on humans.

**Competing interests** The authors have no competing interests or conflicts of interest to declare that are relevant to the contents of this article

## References

1. Corigliano P, Crupi V, Guglielmino E, Sili AM (2018) Full-field analysis of AL/FE explosive welded joints for shipbuilding applications. *Mar Struct* 57:207–218. <https://doi.org/10.1016/j.marstruc.2017.10.004>
2. Crossland B (1982) Explosive welding of metals and its application. (Book). Oxford Ser Adv Manuf 2:233
3. Findik F (2011) Recent developments in explosive welding. *Mater Des* 32(3):1081–1093. <https://doi.org/10.1016/j.matdes.2010.10.017>
4. Kaya Y (2018) Microstructural, mechanical and corrosion investigations of ship steel-aluminum bimetal composites produced by explosive welding. *Metals* 8(7):544. <https://doi.org/10.3390/met8070544>
5. Tayebi P, Fazli A, Asadi P, Soltanpour M (2019) Formability analysis of dissimilar friction stir welded AA 6061 and AA 5083 blanks by SPIF process. *CIRP J Manuf Sci Technol* 25:50–68. <https://doi.org/10.1016/j.cirpj.2019.02.002>
6. Wronka B (2011) Testing of explosive welding and welded joints. Wavy character of the process and joint quality. *Int J Impact Eng* 38(5):309–313. <https://doi.org/10.1016/j.ijimpeng.2010.11.003>
7. Guo X, Wang H, Liu Z, Wang L, Ma F, Tao J (2016) Interface and performance of CLAM steel/aluminum clad tube prepared by explosive bonding method. *Int J Adv Manuf Technol* 82(1–4):543–548. <https://doi.org/10.1007/s00170-015-7380-z>
8. Durgutlu A, Okuyucu H, Gulenc B (2008) Investigation of effect of the stand-off distance on interface characteristics of explosively welded copper and stainless steel. *Mater Des* 29(7):1480–1484. <https://doi.org/10.1016/j.matdes.2007.07.012>
9. Bina MH, Dehghani F, Salimi M (2013) Effect of heat treatment on bonding interface in explosive welded copper/stainless steel. *Mater Des* 45:504–509. <https://doi.org/10.1016/j.matdes.2012.09.037>
10. Acarer M, Gülenç B, Findik F (2004) The influence of some factors on steel/steel bonding quality on there characteristics of explosive welded joints. *J Mater Sci* 39(21):6457–6466. <https://doi.org/10.1023/B:JMSSC.0000044883.33007.20>
11. Yuce C, Karpat F, Yavuz N (2019) Investigations on the microstructure and mechanical properties of laser welded dissimilar galvanized steel–aluminum joints. *Int J Adv Manuf Technol* 104(5–8):2693–2704. <https://doi.org/10.1007/s00170-019-04154-7>
12. Paul H, Lityńska-Dobrzyńska L, Prażmowski M (2013) Microstructure and phase constitution near the interface of explosively welded aluminum/copper plates. *Metall Mater Trans A* 44(8):3836–3851. <https://doi.org/10.1007/s11661-013-1703-1>
13. Sherpa BB, Kumar PD, Upadhyay A, Batra U, Agarwal A (2014) Study of the explosive welding process and applications. In: *Advances in applied physical and chemical sciences: a sustainable approach*. Excellent Publishing House, New Delhi, pp 33–39
14. Merriman C (2006) The fundamentals of explosion welding. *Weld J* 85(7):27–29
15. Sherpa BB, Kumar PD, Upadhyay A, Kumar S, Aggarwal A, Tyagi S (2019) Explosive welding of Al-MS plates and its interface characterization. *Explos Shock Waves High Strain Rate Phenom* 13:128. <https://doi.org/10.21741/9781644900338-22>
16. Zeng X-Y, Li X-Q, Li X-J, Mo F, Yan H-H (2019) Numerical study on the effect of thermal conduction on explosive welding interface. *Int J Adv Manuf Technol* 104(5–8):2607–2617. <https://doi.org/10.1007/s00170-019-04054-w>
17. Zhang H, Jiao KX, Zhang JL, Liu J (2018) Microstructure and mechanical properties investigations of copper-steel composite fabricated by explosive welding. *Mater Sci Eng A* 731:278–287. <https://doi.org/10.1016/j.msea.2018.06.051>
18. Bai Q-L, Zhang L-J, Xie M-X, Yang H-X, Zhang J-X (2017) An investigation into the inhomogeneity of the microstructure and mechanical properties of explosive welded H62-brass/Q235B-steel clad plates. *Int J Adv Manuf Technol* 90(5–8):1351–1363. <https://doi.org/10.1007/s00170-016-9440-4>
19. Carvalho G, Galvão I, Mendes R, Leal R, Loureiro A (2019) Weldability of aluminium-copper in explosive welding. *Int J Adv Manuf Technol* 103(5–8):3211–3221. <https://doi.org/10.1007/s00170-019-03841-9>
20. Mali V, Bataev A, Maliutina IN, Kurguzov V, Bataev I, Esikov M, Lozhkin V (2017) Microstructure and mechanical properties of Ti/Ta/Cu/Ni alloy laminate composite materials produced by explosive welding. *Int J Adv Manuf Technol* 93(9–12):4285–4294. <https://doi.org/10.1007/s00170-017-0887-8>
21. Fang Y, Jiang X, Mo D, Zhu D, Luo Z (2019) A review on dissimilar metals' welding methods and mechanisms with interlayer. *Int J Adv Manuf Technol* 102(9–12):2845–2863. <https://doi.org/10.1007/s00170-019-03353-6>

22. Li X, Ma H, Shen Z (2015) Research on explosive welding of aluminum alloy to steel with dovetail grooves. *Mater Des* 87: 815–824. <https://doi.org/10.1016/j.matdes.2015.08.085>
23. Guo X, Fan M, Wang L, Ma F (2016) Bonding interface and bending deformation of Al/316LSS clad metal prepared by explosive welding. *J Mater Eng Perform* 25(6):2157–2163. <https://doi.org/10.1007/s11665-016-2057-9>
24. P. D. Kumar AU, S. Kumar, D. Kanojia, K. Chandra, V., Kain PM, T. Raychaudhuri (2014) Importance of low VoD explosive and characterization of explosive welded joint interface of Al-6061 and SS-304. In: 9th HEMCE-2014, Thiruvananthapuram, Indi
25. Carvalho G, Galvão I, Mendes R, Leal R, Loureiro A (2018) Explosive welding of aluminium to stainless steel. *J Mater Process Technol* 262:340–349. <https://doi.org/10.1016/j.jmatprotec.2018.06.042>
26. Acarer M, Demir B (2008) An investigation of mechanical and metallurgical properties of explosive welded aluminum–dual phase steel. *Mater Lett* 62(25):4158–4160. <https://doi.org/10.1016/j.matlet.2008.05.060>
27. Ming Y, Z-w SHEN, D-g CHEN, Y-x DENG (2019) Microstructure and mechanical properties of Al-Fe meshing bonding interfaces manufactured by explosive welding. *Trans Nonferrous Metals Soc China* 29(4):680–691. [https://doi.org/10.1016/S1003-6326\(19\)64978-2](https://doi.org/10.1016/S1003-6326(19)64978-2)
28. Aceves SM, Espinosa-Loza F, Elmer JW, Huber R (2015) Comparison of Cu, Ti and Ta interlayer explosively fabricated aluminum to stainless steel transition joints for cryogenic pressurized hydrogen storage. *Int J Hydrog Energy* 40(3):1490–1503. <https://doi.org/10.1016/j.ijhydene.2014.11.038>
29. Carvalho G, Galvão I, Mendes R, Leal R, Loureiro A (2020) Explosive welding of aluminium to stainless steel using carbon steel and niobium interlayers. *J Mater Process Technol* 283: 116707. <https://doi.org/10.1016/j.jmatprotec.2020.116707>
30. Shiran MKG, Khalaj G, Pouraliakbar H, Jandaghi M, Bakhtiari H, Shirazi M (2017) Effects of heat treatment on the intermetallic compounds and mechanical properties of the stainless steel 321–aluminum 1230 explosive-welding interface. *Int J Miner Metall Mater* 24(11):1267–1277. <https://doi.org/10.1007/s12613-017-1519-x>
31. Baqer YM, Ramesh S, Yusoff F, Manladan S (2018) Challenges and advances in laser welding of dissimilar light alloys: Al/Mg, Al/Ti, and Mg/Ti alloys. *Int J Adv Manuf Technol* 95(9–12):4353–4369. <https://doi.org/10.1007/s00170-017-1565-6>
32. Carvalho G, Galvão I, Mendes R, Leal R, Loureiro A (2018) Formation of intermetallic structures at the interface of steel-to-aluminium explosive welds. *Mater Charact* 142:432–442. <https://doi.org/10.1016/j.matchar.2018.06.005>
33. Sherpa BB, Kumar PD, Upadhyay A, Kumar S, Aggarwal A, Tyagi S (2020) Low velocity of detonation explosive welding (LVEW) process for metal joining. *Propellants Explos Pyrotech* 45(10): 1554–1565. <https://doi.org/10.1002/prep.202000019>
34. Saravanan S, Raghukandan K (2012) Thermal kinetics in explosive cladding of dissimilar metals. *Sci Technol Weld Join* 17(2):99–103. <https://doi.org/10.1179/1362171811Y.0000000080>
35. Hokamoto K, Izuma T, Fujita M (1993) New explosive welding technique to weld. *Metall Trans A* 24(10):2289–2297. <https://doi.org/10.1007/BF02648602>
36. Acarer M, Gülenç B, Findik F (2003) Investigation of explosive welding parameters and their effects on microhardness and shear strength. *Mater Des* 24(8):659–664. [https://doi.org/10.1016/S0261-3069\(03\)00066-9](https://doi.org/10.1016/S0261-3069(03)00066-9)
37. Mousavi SA, Sartangi PF (2009) Experimental investigation of explosive welding of cp-titanium/AISI 304 stainless steel. *Mater Des* 30(3):459–468. <https://doi.org/10.1016/j.matdes.2008.06.016>
38. Carvalho G, Galvão I, Mendes R, Leal R, Loureiro A (2018) Influence of base material properties on copper and aluminium–copper explosive welds. *Sci Technol Weld Join* 23(6):501–507. <https://doi.org/10.1080/13621718.2017.1417783>
39. Zhang L-J, Pei Q, Zhang J-X, Bi Z-Y, Li P-C (2014) Study on the microstructure and mechanical properties of explosive welded 2205/X65 bimetallic sheet. *Mater Des* 64:462–476. <https://doi.org/10.1016/j.matdes.2014.08.013>
40. Manikandan P, Hokamoto K, Fujita M, Raghukandan K, Tomoshige R (2008) Control of energetic conditions by employing interlayer of different thickness for explosive welding of titanium/304 stainless steel. *J Mater Process Technol* 195(1–3):232–240. <https://doi.org/10.1016/j.jmatprotec.2007.05.002>
41. Akbari-Mousavi S, Barrett L, Al-Hassani S (2008) Explosive welding of metal plates. *J Mater Process Technol* 202(1–3):224–239. <https://doi.org/10.1016/j.jmatprotec.2007.09.028>
42. Bataev I, Lazurenko D, Tanaka S, Hokamoto K, Bataev A, Guo Y, Jorge A Jr (2017) High cooling rates and metastable phases at the interfaces of explosively welded materials. *Acta Mater* 135:277–289. <https://doi.org/10.1016/j.actamat.2017.06.038>
43. Sun Z, Shi C, Wu X, Shi H (2020) Comprehensive investigation of effect of the charge thickness and stand-off gap on interface characteristics of explosively welded TA2 and Q235B. *Compos Interfaces*:1–17. <https://doi.org/10.1080/09276440.2020.1716578>
44. Cui Y, Liu D, Zhang Y, Deng G, Fan M, Chen D, Sun L, Zhang Z (2020) The microstructure and mechanical properties of TA1-low alloy steel composite plate manufactured by explosive welding. *Metals* 10(5):663. <https://doi.org/10.3390/met10050663>
45. Athar MH, Tolaminejad B (2015) Weldability window and the effect of interface morphology on the properties of Al/Cu/Al laminated composites fabricated by explosive welding. *Mater Des* 86: 516–525. <https://doi.org/10.1016/j.matdes.2015.07.114>
46. Kaya Y, Eser G (2019) Production of ship steel—titanium bimetallic composites through explosive cladding. *Weld World* 63(6): 1547–1560. <https://doi.org/10.1007/s40194-019-00771-8>
47. Sherpa BB, Kumar PD, Upadhyay A, Kumar S, Tyagi S (2020) Neuro-fuzzy technique for micro-hardness evaluation of explosive welded joints. *Trans Indian Inst Metals* 73(5):1287–1299. <https://doi.org/10.1007/s12666-020-01980-2>
48. Kahraman N, Gülenç B (2005) Microstructural and mechanical properties of Cu–Ti plates bonded through explosive welding process. *J Mater Process Technol* 169(1):67–71. <https://doi.org/10.1016/j.jmatprotec.2005.02.264>
49. Mastanaiah P, Reddy GM, Prasad KS, Murthy C (2014) An investigation on microstructures and mechanical properties of explosive clad C103 niobium alloy over C263 nimonic alloy. *J Mater Process Technol* 214(11):2316–2324. <https://doi.org/10.1016/j.jmatprotec.2014.04.025>
50. Fang Z, Shi C, Shi H, Sun Z (2019) Influence of explosive ratio on morphological and structural properties of Ti/Al clads. *Metals* 9(2): 119. <https://doi.org/10.3390/met9020119>
51. Wang J, Zhang P, Duan Q, Yang G, Wu S, Zhang Z (2010) Tensile deformation behaviors of Cu–Ni alloy processed by equal channel angular pressing. *Adv Eng Mater* 12(4):304–311. <https://doi.org/10.1002/adem.200900281>
52. Yang M, Ma H, Shen Z, Sun Y (2019) Study on explosive welding for manufacturing meshing bonding interface of CuCrZr to 316L stainless steel. *Fusion Eng Des* 143:106–114. <https://doi.org/10.1016/j.fusengdes.2019.03.137>